The Astrophysical Journal, 763:19 (8pp), 2013 January 20 doi:10.1088/0004-637X/763/1/19

EXACT SOLUTION TO FINITE TEMPERATURE SFDM: NATURAL CORES WITHOUT FEEDBACK

Victor H. Robles and T. Matos
Departamento de Física, Centro de Investigación y de Estudios Avanzados del IPN, AP 14-740, 0700 D.F., México, Mexico;
vrobles@fis.cinvestav.mx, tmatos@fis.cinvestav.mx
Received 2012 August 6; accepted 2012 November 11; published 2012 December 28

ABSTRACT

Recent high-quality observations of low surface brightness (LSB) galaxies have shown that their dark matter (DM) halos prefer flat central density profiles. However, the standard cold dark matter model simulations predict a more cuspy behavior. One mechanism used to reconcile the simulations with the observed data is the feedback from star formation. While this mechanism may be successful in isolated dwarf galaxies, its success in LSB galaxies remains unclear. Additionally, the inclusion of too much feedback in the simulations is a double-edged sword—in order to obtain a cored DM distribution from an initially cuspy one, the feedback recipes usually require one to remove a large quantity of baryons from the center of the galaxies; however, some feedback recipes produce twice the number of satellite galaxies of a given luminosity and with much smaller mass-to-light ratios from those that are observed. Therefore, one DM profile that produces cores naturally and that does not require large amounts of feedback would be preferable. We find both requirements to be satisfied in the scalar field dark matter model. Here, we consider that DM is an auto-interacting real scalar field in a thermal bath at temperature T with an initial Z_2 symmetric potential. As the universe expands, the temperature drops so that the Z_2 symmetry is spontaneously broken and the field rolls down to a new minimum. We give an exact analytic solution to the Newtonian limit of this system, showing that it can satisfy the two desired requirements and that the rotation curve profile is no longer universal.

Key words: galaxies: formation – galaxies: fundamental parameters – galaxies: halos – galaxies: individual (NGC 1003, NGC 1560, NGC 6946)

Online-only material: color figures

1. INTRODUCTION

The longstanding core/cusp discussion on whether the central dark matter (DM) profiles in dwarfs and low surface brightness (LSB) galaxies are more core-like and rounder than the standard cold dark matter (CDM) model predicts remains an open issue (van Eymeren et al. 2009; see de Blok 2010 for a recent review). Thus far, the core profiles most frequently used in the literature and that best fit the observations are empirical (Burkert 1995; Kuzio de Naray et al. 2010). Though they are useful to characterize the properties of galaxies, it is necessary to find a theoretical framework that naturally produces the cores, especially since an increasing number of recent high-quality observations of LSB galaxies suggest that a core-like behavior ($\rho \sim r^{-0.2}$) is preferred in the central regions of dwarf and LSB galaxies (Oh et al. 2011; Robles & Matos 2012; de Blok et al. 2001). This is a problem for the CDM model, which prefers $\rho \sim r^{-1}$ at small r (Navarro et al. 2010). However, the latest simulations can reach $\rho \sim r^{-0.8}$ (Navarro et al. 2010; Merrit et al. 2006; Graham et al. 2006), which is not in total agreement with observations. The current trend for solving the core/cups discrepancy in the CDM model is to include the dynamics of the baryonic component in DM simulations (Governato et al. 2010, 2012; Macciò et al. 2012; Stinson et al. 2012; Romano-Díaz et al. 2008). By including feedback from star formation in simulations of field dwarf galaxies, Governato et al. (2012) managed to change an initially cuspy DM halo into a core-like halo. However, it still remains to be seen if the same feedback recipes used in dwarf galaxies work as well in massive LSBs. As pointed out in Kuzio de Naray & Spekkens (2011), this seems unlikely, though it is necessary to show that there is an accord between the surface gas density in LSBs and the amount of surface gas obtained in CDM simulations (Brook et al. 2012; Stinson et al. 2012; Guo et al. 2010; More et al. 2011; Kuzio de Naray & Kaufmann 2011). We know that LSBs are a large portion of the total galaxies that are observed (McGaugh et al. 1995); therefore, as there is no agreement yet between LSBs and CDM simulations it is worth exploring alternative models.

Another problem is that Sawala et al. (2012) find in their simulations twice as many satellites of a given luminosity around a Milky-Way-size host halo and found that, if galaxies are intrinsically cored at infall then the transition from high gas mass irregulars to dwarf spheroidals cannot be only due to tidal stripping. They found this by considering, in addition to feedback, the effect that surrounding galaxies have on its host halo by means of tidal interaction. They find that the DM halos of satellites are more strongly affected than their stellar component by tidal interactions and conclude from their simulations that it is difficult to reconcile the observed high total mass-to-light ratios in dwarf spheroidal galaxies (dSphs) with those found on their simulated counterparts under the CDM paradigm. A solution to this discrepancy should also be addressed in any alternative DM model.

There are several models in the literature that address these and some other problems (Avila-Reese et al. 2001; Cembranos et al. 2005; Strigari et al. 2007; Spergel & Steinhardt 2000; Magaña & Matos 2012). Models that slightly modify CDM, such as the warm dark matter (WDM) and self-interacting dark matter (SIDM) models, have not yet been able to solve these discrepancies (Villaescusa & Dalal 2011; Kuzio de Naray & Spekkens 2011; Zavala et al. 2009; Davé et al. 2001; Yoshida et al. 2000). There are models that modify gravity, such as $f(R)$ theories (De Felice & Tsujikawa 2010) and MOND (Milgrom 2010; Sanders 2009), but they are currently more at the effective-theory level rather than at a fundamental one. Nevertheless, there are some rotation curve fits of LSBs galaxies in MOND models

whose fits are almost in perfect agreement with the observed data, for instance, NGC 1560 (Sanders 2009).

One model that has received much attention is the scalar field dark matter (SFDM) model. It is our aim to show that in this model there is a scenario of galaxy formation (described in Section 2) different from the standard model used in CDM simulations and that naturally produces core density profiles, reproducing rotation curves of large and small galaxies on equal footing as MOND and empirical DM models do, but that may not need large amounts of feedback to agree with observations.

In previous works, it has been verified that the SFDM model reproduces cosmological observations as well as CDM (Rodríguez-Montoya et al. 2010; Suárez & Matos 2011; Magaña & Matos 2012; Harko 2011). On cosmological scales, choosing a scalar field mass of $m \sim 10^{-22}$ eV$/c^2$ gives the same cosmological density evolution as CDM (Matos et al. 2009; Chavanis 2011) and is consistent with the acoustic peaks of the cosmic microwave background radiation (Rodríguez-Montoya et al. 2010). Moreover, Matos & Ureña (2001) and Hu et al. (2000) found that it suffices that $m < 10^{-17}$ eV$/c^2$ for the Scalar Field (SF) to condensate. On the small-scale regime, Rindler-Daller & Shapiro (2012) studied the formation of the vortex in SFDM halos and found that constraints on the boson mass were in agreement with previous works (Kain & Ling 2010; Zinner 2011). Lora et al. (2012) analyzed the dynamics of Ursa Minor and its stellar clump within the SFDM paradigm and found a good agreement with observations where $m \sim 10^{-22}$ eV$/c^2$. On a galactic scale, self-interaction plays an important role; however, its constraints are still not very tight, especially since the interaction parameter always appears entangled with m when fitting the rotation curves (Robles & Matos 2012; Böhmer & Harko 2007). The existence of two parameters allows us to use a smaller value for the SF mass (Böhmer & Harko 2007; Harko 2011); nevertheless, $m \sim 10^{-22}$ eV$/c^2$ is also possible, therefore, there is no incompatibility with cosmological and galactic scale parameters.

The paper is organized as follows. In Section 2 we describe the SFDM model to be analyzed in this paper, in Section 3 we give our results, and in Section 4 we give our conclusions.

2. SFDM MODEL

2.1. Previous Work and Unsolved Issues

The idea that DM is a scalar field was first considered by Sin (1994) and independently introduced by Guzmán & Matos (2000). In the SFDM model, the main hypothesis is that DM is an auto-interacting real SF that condensates forming Bose–Einstein Condensate (BEC) "drops" (Magaña & Matos 2012). We interpret these BEC drops to be the halos of galaxies, such that their wave properties and the Heisenberg uncertainty principle stop the DM phase-space density from growing indefinitely, and thus, it avoids cuspy halos and reduces the number of small satellites (Hu et al. 2000).

In the SFDM model, the scenario of galaxy formation proposes that galactic halos form from the condensation of an SF with an ultra-light mass of the order of $m \sim 10^{-22}$ eV (units where the speed of light $c = 1$). From this mass, it follows that the critical temperature of the condensation in the SF is $T_{\rm crit} \sim m^{-5/3} \sim$ TeV, which is very high. Thus, BEC drops are formed very early in the universe. It has been proposed that these drops are the halos of galaxies (Matos & Ureña 2001), i.e., that halos are gigantic clumps of SF.

The DM halos of galaxies can be described in the non-relativistic regime, where they can be seen as Newtonian gas. When the SF has self-interaction, we need to add a quartic term to the SF potential, and in the Newtonian limit, the equation of state of the SF is that of a polytrope of index 1 (Suárez & Matos 2011; Harko 2011). Some studies of the stability of these SF configurations have shown that stable large-scale configurations are not preferred (Colpi et al. 1986; Balakrishna et al. 1998; Valdez et al. 2011). Though the critical mass for stability depends on which parameter values were used, all reach the same conclusion, that very large configurations, like those of cluster scales (masses of $M \geqslant 10^{13}\ M_\odot$), are usually unstable. Therefore, these structures were most likely to form just as in the CDM model—by hierarchy (Matos & Ureña 2001; Suárez & Matos 2011), i.e., by mergers of smaller halos. The concept behind the SFDM model is as follows: after inflation big structures start to grow hierarchically, as in the CDM model, and its growth is then boosted by the SB mechanism. Inside these structures, galactic sized halos will form by condensation. Thus, all predictions of the CDM model at large scales are reproduced by SFDM (Colpi et al. 1986; Gleiser 1988; Matos & Ureña 2001; Chavanis 2011). Although the model is quite successful, there are at least two reasons why the model must be complemented in addition to finding an explanation to the two discrepancies discussed in the Introduction.

The first discrepancy is found when we consider the fully condensed system at temperature $T = 0$. The fits to the rotation curves (RCs) of the LSBs (Robles & Matos 2012; Böhmer & Harko 2007) show deviations from the observed data at large radii because the DM halos are modeled by only considering the ground state (complete condensation), the DM density of which and velocity profile are given by (Böhmer & Harko 2007)

$$\rho^0(r) = \rho_0^0 \frac{\sin(\pi r/\hat{R})}{\pi r/\hat{R}}, \tag{1a}$$

$$V_0^2(r) = \frac{4\pi G \rho_0^0}{K^2}\left(\frac{\sin(Kr)}{Kr} - \cos(Kr)\right), \tag{1b}$$

where $K = \pi/\hat{R}$, $\rho_0^0 = \rho^0(0)$ is the central density, and the halo radius determined by $\rho(\hat{R}) = 0$ is

$$\hat{R} = \pi\sqrt{\frac{\hbar^2 b}{Gm^3}}. \tag{2}$$

Here, $\hbar$ is Planck's constant divided by 2π, m is the mass of the DM particle, G is the gravitational constant, and b is the scattering length. The latter is related to the coupling constant λ' by $\lambda' = 4\pi\hbar^2 b/m$. The density profile depends on two fitting parameters, the central density and a length scale $\hat{R}$. However, $\hat{R}$ depends only on fixed parameters, the interaction parameter λ' and the mass of the SF particle, which implies that it should not vary from galaxy to galaxy. However, when fitting the rotation curves of galaxies, as $\hat{R}$ is a fitting parameter, it has different values for each galaxy (Robles & Matos 2012; Böhmer & Harko 2007). This is somewhat contradictory and represents a problem for the simplest SFDM model.

The second problem lies in the rapid decrease of the velocity profile (Equation (1b)) after its maximum value. Such a decrease causes a disagreement between the fits and the observed data in large galaxies because the data usually remain "flat" until the outermost regions (Swaters et al. 2000). In addition to this, and for large galaxies, when we aim for the best fit to the velocity

maximum, we obtain a worse fit in the outer regions, i.e., the better the fit to the velocity maximum in the RC, the worse the fit becomes in the outer regions and vice versa.

One approach to solving those problems was considered by Matos & Ureña (2007) and later by Harko & Madarassy (2011). It consisted of including the finite temperature of the DM in the DM halos. Harko & Madarassy (2011) show that by including a small correction to the pure condensed state, albeit in a different way from the one in this paper, it is possible to solve the first discrepancy and to partially solve the second one. The inclusion of temperature T mainly does two things: (1) it makes the halo radius temperature dependent, thus it is no longer fixed for all galaxies and (2) it lifts the RC fit in the outer region and keeps it flat until the last value. However, the consequence of (2) is negligible when the halo temperature is $T < 0.5\ T_{\rm BEC}$, where $T_{\rm BEC}$ is the critical temperature of the Bose–Einstein condensation. If $T_{\rm BEC} \sim$ TeV ($c = 1$), then we would expect that the present halos would be well approximated by Equation (1b) and hence, we would be unable to simultaneously obtain a good fit to the RC maximum and the RC outer regions. Though this last problem is not readily visible in galaxies with a small radius (outer radius of $\leqslant$10 kpc), it is conspicuous in large galaxies, therefore problem (2) is only partially solved.

Thus, an alternative approach to solving these two SFDM discrepancies considers the non-condensed SF configurations at $T = 0$, i.e., SF configurations in excited states (Balakrishna et al. 1998; Ureña & Bernal 2010; Bernal et al. 2010). These configurations fit RCs up to the last data point and can even reproduce the wiggles seen at large radii in high-resolution observations (Sin 1994; Colpi et al. 1986). The problem found in this kind of solution was that the configurations required for good fits (4-5 exited states) were unstable and decayed to the ground state in a short time (Siddhartha & Ureña 2003). Therefore, we will expect to see that most DM halos are in their ground state, which means that the disagreement at large radii would remain.

2.2. Finite Temperature SF Scenario

Motivated to solve all these issues, we consider the following scenario that includes the temperature of the DM and the excited states of the SF.

The idea is that the DM is a spin 0 scalar field Φ, with a repulsive interaction embedded in a thermal bath of temperature T; we also consider the finite temperature corrections up to one loop in the perturbations. This system is described by the potential (Kolb & Turner 1987; Dalfovo et al. 1999)

$$V(\Phi) = -\frac{1}{2}\frac{\hat{m}^2c^2}{\hbar^2}\Phi^2 + \frac{\hat{\lambda}}{4}\Phi^4 + \frac{\hat{\lambda}}{8}k_{\rm B}^2T^2\Phi^2 - \frac{\pi^2k_{\rm B}^4T^4}{90\hbar^2c^2}, \quad (3)$$

for the case when $k_{\rm B}T \gg \hat{m}c^2$. Here, $k_{\rm B}$ is Boltzmann's constant, $\hat{\lambda} = \lambda/(\hbar^2c^2)$ is the parameter describing the interaction, $\hat{\mu}^2 := \hat{m}^2c^2/\hbar^2$ is a parameter, and T is the temperature of the thermal bath. The first term in $V(\Phi)$ relates to the mass term, the second to the repulsive self-interaction, the third to the interaction of the field with the thermal bath, and the last to the thermal bath alone.

At some high-enough temperature in the early universe, the SF interacts with the rest of the matter; however, due to the expansion of the universe, its temperature will keep decreasing. Eventually, when the temperature is sufficiently small, the SF decouples from the interaction with the rest of the matter and follows its own thermodynamic history, while the background keeps cooling down due to the expansion. Moreover, as the temperature continues decreasing, the field will reach the minimum of the potential $\Phi \approx 0$. This initial minimum of the potential eventually becomes a local maximum and after this moment, the initial Z_2 symmetry of the potential $V(\Phi)$ will be broken. The latter happens at a critical temperature T_C given by

$$k_{\rm B}T_C = \frac{2\hat{m}c^2}{\sqrt{\lambda}}. \quad (4)$$

We will see that the critical temperature determines the moment at which the DM fluctuations can start growing. They grow from the moment when $T < T_C$ until they reach a stable equilibrium point, for example, in $\Phi^2_{\rm min} = k_{\rm B}^2(T_C^2 - T^2)/4$ (see Section 2.3).

2.3. Evolution Equations

The perturbed system of a scalar field with a quartic repulsive interaction and with temperature of zero has been studied before (Colpi et al. 1986; Ureña & Bernal 2010). Following the same procedure, we study the evolution of the SF in an FRW universe. We write the metric tensor as $\mathbf{g} = \mathbf{g}^0 + \delta\mathbf{g}$, where $\mathbf{g}^0$ is the unperturbed FRW background metric and $\delta\mathbf{g}$ is the perturbation. The perturbed line element in conformal time η is (we take $c = 1$ in this subsection)

$$ds^2 = a(\eta)^2(-(1+2\psi)d\eta^2 + 2B_{,i}\,d\eta dx^i + a(\eta)^2[(1-2\phi)\delta_{ij} + 2E_{,ij}]dx^i dx^j, \quad (5)$$

with a being the scale factor, ψ the lapse function, ϕ gravitational potential, B the shift, and E the anisotropic potential. We separate the energy–momentum tensor and the field as $\mathbf{T} = \mathbf{T}_0 + \delta\mathbf{T}$ and $\Phi(x^\mu) = \Phi_0(\eta) + \delta\Phi(x^\mu)$, respectively. As we are studying the linear regime $\delta\Phi(x^\mu) \ll \Phi_0(\eta)$, we can approximate $V(\Phi) \approx V(\Phi_0)$. We work in the Newtonian gauge where the metric tensor $\mathbf{g}$ becomes diagonal and as a result, in the trace of Einstein's equations, the scalar potentials ψ and ϕ are identical, therefore; ψ relates to the gravitational potential.

Changing to the cosmological time t when using the relation $(d/d\eta) = a(d/dt)$, the perturbed Einstein's equations $\delta G^i_j = 8\pi G\delta T^i_j$ to first order for a scalar field in the Newtonian gauge ($E = 0 = B$) are

$$-8\pi G\delta\rho_\Phi = 6H(\dot{\phi} + H\phi) - \frac{2}{a^2}\nabla^2\phi, \quad (6a)$$

$$8\pi G\dot{\Phi}_0\delta\Phi_{,i} = 2(\dot{\phi} + H\phi)_{,i}, \quad (6b)$$

$$8\pi G\delta p_\Phi = 2[\ddot{\phi} + 3H\dot{\phi} + (2\dot{H} + H^2)\phi] \quad (6c)$$

with $\dot{} = \partial/\partial t$ and $H = d(\ln a)/dt$: The perturbed density $\delta\rho_\Phi$ and the perturbed pressure δp_Φ are defined in terms of the perturbed energy momentum tensor as

$$\begin{aligned}\delta T^0_0 &= -\delta\rho_\Phi = -\left(\dot{\Phi}_0\delta\dot{\Phi} - \dot{\Phi}_0^2\psi + V_{,\Phi_0}\delta\Phi\right),\\ \delta T^0_i &= -\frac{1}{a}(\dot{\Phi}_0\delta\Phi_{,i}),\\ \delta T^i_j &= \delta p_\Phi = \left(\dot{\Phi}_0\delta\dot{\Phi} - \dot{\Phi}_0^2\psi - V_{,\Phi_0}\delta\Phi\right)\delta^i_j. \end{aligned} \quad (7)$$

The systems of equations (6) and (7) describe the evolution of the scalar perturbations. To study the evolution of the SF perturbations, we use the perturbed Klein–Gordon equation

$$\delta\ddot{\Phi} + 3H\delta\dot{\Phi} - \frac{1}{a^2}\nabla^2\delta\Phi + V_{,\Phi_0\Phi_0}\delta\Phi + 2V_{,\Phi_0}\phi - 4\dot{\Phi}_0\dot{\phi} = 0. \quad (8)$$

Equation (8) can be rewritten as

$$\Box\delta\Phi + \left.\frac{d^2V}{d\Phi^2}\right|_{\Phi_0}\delta\Phi + 2\left.\frac{dV}{d\Phi}\right|_{\Phi_0}\phi - 4\dot{\Phi}_0\dot{\phi} = 0, \quad (9)$$

where the D'Alambertian operator is defined as

$$\Box := \frac{\partial^2}{\partial t^2} + 3H\frac{\partial}{\partial t} - \frac{1}{a^2}\nabla^2. \quad (10)$$

Essentially Equation (8) represents a harmonic oscillator with a damping of $3H\delta\dot{\Phi}$ and an extra force of $-2\phi V_{,\Phi_0}$. Equation (8) has oscillating solutions if $(V_{,\Phi\Phi} - (1/a^2)\nabla^2)\delta\Phi$ is positive. This equation contains growing solutions if this term is negative, that is, if $V_{,\Phi\Phi}$ is negative enough. From here, we see an important feature. These perturbations grow only if V has a maximum, even if it is a local one. Here, the potential is unstable and during the time when the scalar field remains at the maximum, the scalar field fluctuations grow until they reach a new stable point. If we use Equation (3) the transition from a local minimum to a local maximum happens when $T = T_C$, thus, we see why T_C determines the moment in which the DM fluctuations can start growing. This implies that the galactic scale halos could have formed within this period and with similar features. Finally for the background field equation we assume that $\phi \approx 0$, therefore its equation reads

$$\ddot{\Phi}_0 + 3H\dot{\Phi}_0 + V_{,\Phi}(\Phi_0) = 0. \quad (11)$$

Φ_0 depends only on time.

We now suppose that the temperature is sufficiently small, such that the interaction between the SF and the rest of matter has decoupled—after this moment the field stops interacting with the rest of the particles. We also assume that the symmetry break (SB) took place in the radiation-dominated era in a flat universe. We mentioned that after the SB, the perturbations can grow until they reach their new minimum, thus, each perturbation has a temperature at which it forms and separates from the background field following its own evolution. We denote this temperature of formation by $T_\Phi := T(t_{\rm form})$, where $t_{\rm form}$ is the time in which the halo forms. Under these assumptions the equation for an SF perturbation which is formed at T_Φ reads

$$\Box\delta\Phi + \frac{\hat{\lambda}}{4}\left[k_{\rm B}^2(T_\Phi^2 - T_C^2) + 12\Phi_0^2\right]\delta\Phi - 4\dot{\Phi}_0\dot{\phi} + \frac{\hat{\lambda}}{2}\left[k_{\rm B}^2(T_\Phi^2 - T_C^2) + 4\Phi_0^2\right]\Phi_0\phi = 0. \quad (12)$$

In Figure 1, we show the behavior of the potential for different temperatures, and we see that the SB takes place at $T = T_C$.

In the SFDM model, the initial fluctuations come from inflation as in the standard CDM paradigm. Later on the field decouples from the rest of the matter and goes through an SB which can increase the fluctuation's amplitude, forming the initial structures of the universe.

In this work, as one of our main interests' is to find an exact analytical solution to Equation (12). We will not pursue the task of solving it numerically here. However, the numerical work done in Magaña & Matos (2012) has confirmed that the behavior of the SF perturbation just after the SB is what we had expected from our analysis of Equation (9). They have analyzed in some detail the evolution of a perturbation with a wavelength of 2 Mpc and a density contrast of $\delta = 1 \times 10^{-7}$ after the SB. They took

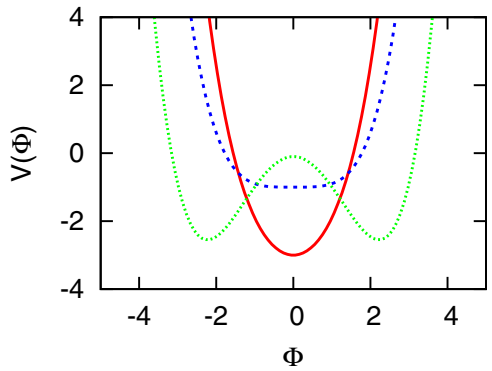

Figure 1. Qualitative behavior of $V(\Phi)$ vs. Φ for three different values of T. The solid line (red in the online version) is where $T > T_C$. Here the system oscillates around the minimum and possesses a Z_2 symmetry. The dashed line (Blue in the online version) is where the SB takes place, which happens when $T = T_C$. The dotted line (green in the online version) is for $T < T_C$; in this period Φ can roll down to a new minimum and there is no longer Z_2 symmetry. (A color version of this figure is available in the online journal.)

$a = 10^{-6}$ as an initial condition and evolved it until $a = 10^{-3}$. They also analyzed the case where $T \sim T_C$ and showed that as the temperature decreases and goes below T_C, Φ_0 falls rapidly to a new minimum, where it remains oscillating. Meanwhile, the SF fluctuation grows quickly as Φ_0 approaches the new minimum. It is only before the SB that the SF remains homogeneous.

From here we see that in the SFDM model, the primordial DM halos form almost at the same time due to the phase transition produced by the SB. In the nonlinear regime, these halos can merge with other halos, forming larger structures just as in the CDM model. Therefore, one of the main differences with the CDM model lies in the initial formation of the DM halos, where they are formed very rapidly and almost at the same time. From this we expect that they possess similar features. This difference between the SFDM and CDM models can be tested by observing well-formed high-redshift galaxies and also by comparing the characteristic parameters of several DM dominated systems, for example, by observing that indeed, dwarf or LSB galaxies possess cores even at high redshift, especially since the CDM simulations of dwarf galaxies by Governato et al. (2012) suggest that their DM density profiles were initially cuspy, but later turn into core profiles due to feedback processes.

2.4. Newtonian Limit

In this work, we are interested in the galactic scale of DM halos after their formation. Thus, we constrain ourselves to solve the Newtonian limit of Equation (12), when Φ is near the minimum of the potential and after the SB, where we expect it to be stable. In this limit, we also expect the gravitational potential to be locally very homogeneous in the beginning of its collapse, thus, $\dot{\phi} \approx 0$. The stability of these halos will be shown elsewhere. For clarity, from here on we stop using units in which $c = 1$. We now find an exact spherically symmetric solution for the SF when it is near the minimum of the potential ($V'(\Phi)|_{\Phi_0} \approx 0$), i.e., when $\Phi_0^2 = \Phi_{\rm min}^2 = k_{\rm B}^2(T_C^2 - T_\Phi^2)/4$ and $T_\Phi < T_C$. For the Newtonian case $H = 0$, $\dot{\Phi}_0 \approx 0$, and Equation (12) reads

$$\delta\ddot{\Phi} - \nabla^2\delta\Phi + \frac{\lambda k_{\rm B}^2}{2\hbar^2}\left(T_C^2 - T_\Phi^2\right)\delta\Phi = 0. \quad (13)$$

Equation (13) describes the evolution of the SF fluctuation, which formed at T_Φ after the SB. Moreover, this equation is linear. In general, halos can evolve with different histories depending on their environment, star formation, gas accretion, and other secular processes that occur in the hosted galaxy. Thus, in order to study these systems in detail, we will need the full nonlinear regime. However, we can still regard Equation (13) as a first approximation for those halos of isolated galaxies or of galaxies that are not heavily influenced by their neighbors, for example, isolated galaxies or galaxies that are in low-mass density regions can be well described by this equation. This is mainly because their halo profiles are not expected to be affected substantially by their initial profiles during their evolution. Furthermore, we expect that the galaxies remain in the Newtonian gravitational regime, thus we can consider that the linear approximation is sufficient for describing a galaxy. Therefore, we interpret a solution of this system as the temperature-corrected density profile of early DM halos.

We find that the ansatz

$$\delta\Phi = \delta\Phi_0 \frac{\sin(kr)}{kr}\cos(\omega t) \tag{14}$$

is an exact solution to Equation (13) provided that

$$\omega^2 = k^2c^2 + \frac{\lambda k_{\rm B}^2}{2\hbar^2}\left(T_C^2 - T_\Phi^2\right). \tag{15}$$

Here, $\delta\Phi_0$ is the amplitude of the fluctuation. From Equation (15) we note that now $k = k(T_\Phi)$. For an easier comparison with the observations, we use the standard definition of number density $n(x,t) = \kappa(\delta\Phi)^2$, where κ is a constant that gives us the necessary units so that we can interpret $n(x,t)$ as the number density of DM particles, as Φ has energy units. With this in mind, we can define an effective mass density of the SF fluctuation as $\rho = mn$ and a central density by $\rho_0 = m\kappa(\delta\Phi_0)^2$. It is important to note that while $\delta\Phi_0$ is not obtained directly from observations, the value of ρ_0 is a direct consequence of the RC fit, and for this reason, it is preferable to work with ρ_0 instead of $\delta\Phi_0$.

Combining Equation (14) and the definition of n we obtain a finite temperature density profile

$$\rho(r) = \rho_0 \frac{\sin^2(kr)}{(kr)^2}, \tag{16}$$

provided that

$$k_{\rm B}^2 T_\Phi^2 = k_{\rm B}^2 T_C^2 - 4\Phi_0^2, \tag{17}$$

$$\Phi_0^2 = \Phi_{\rm min}^2. \tag{18}$$

Here, $k(T_\Phi)$ and $\rho_0 = \rho_0(T_\Phi)$ are fitting parameters while λ, T_C (or m), and κ are free parameters to be constrained by observations.

For galaxies the Newtonian approximation provides a good description; therefore, from Equation (16), we obtain the mass and rotation curve velocity profiles

$$M(r) = \frac{4\pi\rho_0}{k^2}\frac{r}{2}\left(1 - \frac{\sin(2kr)}{2kr}\right), \tag{19a}$$

$$V^2(r) = \frac{4\pi G\rho_0}{2k^2}\left(1 - \frac{\sin(2kr)}{2kr}\right), \tag{19b}$$

respectively. For comparison, we give the Einasto rotation curve profile, which lately seems to give a better description of DM halos in CDM simulations (Navarro et al. 2010; Merrit et al. 2006; Graham et al. 2006),

$$V_{\rm E}^2 = 4\pi G\rho_{-2}\frac{r_{-2}^3}{r}\left[\frac{e^{2/\alpha}}{\alpha}\left(\frac{\alpha}{2}\right)^{(3/\alpha)}\gamma\left(\frac{3}{\alpha}, x'\right)\right], \tag{20}$$

with γ being the incomplete gamma function given by

$$\gamma\left(\frac{3}{\alpha}, x'\right) = \int_0^{x'} e^{-\tau}\,\tau^{(3/\alpha)-1}d\tau$$

where $x' = (2/\alpha)(r/r_{-2})^\alpha$, r_{-2} is the radius in which the logarithmic slope of the density is -2, ρ_{-2} is the density at the radius r_{-2}, and α is the parameter that describes the degree of curvature of the profile (Merrit et al. 2006; Graham et al. 2006).

We now define the radius R of the SFDM distribution using the condition $\rho(R) = 0$. This fixes the relation

$$k_j{\rm R} = j\pi, \quad j = 1, 2, 3, ..., \tag{21}$$

where j is the number of the excited states required to fit a galaxy RC up to the last measured point. From Equations (13), (14), and (21) we find that the halo allows excited states, i.e., the excited states are also solutions of Equation (13). As this equation is linear, there can be halos in a combination of excited states: For these cases, the total density $\rho_{\rm tot}$ is the sum of the densities in the different states

$$\rho_{\rm tot} = \sum_j \rho_0^j \frac{\sin^2(j\pi r/{\rm R})}{(j\pi r/{\rm R})^2}, \tag{22}$$

with ρ_0^j being the central density of the state j. It is important to note that there is only one halo formation temperature, T_Φ, and that the number of states that compose one DM halo depends on each halo—one reason for this is that the initial conditions change from one to another. Finally, we note that for each state j, there exists both ω_j and k_j, which satisfy their corresponding Equation (15).

An additional feature of Equation (16) is the presence of "wiggles." These oscillations are characteristic of SF configurations in excited states, which were also seen in Sin (1994). Also, we define the distance where the first peak (maximum) in the RC is reached as $r_{\rm max}^1$. This determines the first local maximum of the RC velocity, which can be obtained from Equation (23)

$$\frac{\cos(2\pi jy)}{2(\pi j)^2 y}\left[\frac{\tan(2\pi jy)}{2\pi jy} - 1\right] = 0, \tag{23}$$

where we used Equation (21) and $y := (r_{\rm max}^1/{\rm R})$.

3. DISCUSSION

We have seen that within our scenario of DM and galaxy formation, the DM halos are naturally cored, i.e., their central density profiles are finite and do not diverge. On the contrary, they behave as $\rho \sim r^0$ for small r: It is important to note that the core is obtained from the model and not assumed, thus, this is an alternative way to solve the cusp/core discrepancy without adding large amounts of baryons in simulations (Kuzio de Naray & Kaufmann 2011).

In the SFDM model the big DM halos (density fluctuations) form after the SB and grow only after the field rolls to the minimum of the potential, the same potential that varies with the temperature. Nevertheless, during this time the halos are not in thermal equilibrium, and locally the temperature is different from place to place. Therefore, the initial size of the condensation depends on the local halo temperature. From Equations (15) and (21) we see that the size of the DM configuration, specified by R, is now temperature dependent. Therefore, as in Harko & Madarassy (2011), we also solve the problem of having a unique scale length for all halos, but now in a new way, using the SB mechanism. Therefore, different formation temperatures of galactic halos may result in different DM halo sizes.

In Figure 2, we show the RC fits of three galaxies using the minimum disk hypothesis (neglecting the baryonic component) taken from a high-precision subsample of McGaugh (2005) combined with Broeils (1992) for NGC 1560. The sample given in McGaugh (2005) consists of resolved rotation velocity measurements, with an accuracy of 5% or better. The error bars in NGC 1560 are taken from the data in Broeils (1992) and we give a uniform weight of 5% to the other two galaxies. We compare Equation (19b) (solid line) with Equation (20) (dashed line) and note that these galaxies present two features—long flat tails in the outer region and wiggles, though the latter are still debated and a much larger sample is needed to verify their existence in RCs. However, in our sample, they do seem to be present, even after overestimating the error bars. The wiggles (small oscillations) are perfectly reproduced by the SFDM model using combinations of excited states, and the value of j that appears in the panels of Figure 2 specifies the required combination of states for the fit shown. It is important to highlight the SFDM fit of NGC 1560, we note it is as accurate as the one displayed in MOND models (Gentile et al. 2010; Sanders 2009). This combination of states in our RC fits suggests that there is no universal DM profile. Some reasons for this could be that (1) the subsequent evolution determines the final profile, as happens with CDM halos, (2) a collision of two halos with different states formed a halo with the combination of states that we observe today, and (3) the halo formed with the currently observed states and has remained unaltered for a long time. Further research is necessary to determine the most likely explanation.

As for the observed long flat tails, we have noted that the flat outermost region is a consequence of considering excited states, the same behavior that was present in previous works (Sin 1994; Bernal et al. 2010) that used $T = 0$. However, the main difference now is that by considering $T \neq 0$ we can accommodate excited states in halos and expect them to be stable due to the DM thermal and repulsive self-interactions. Moreover, by considering for the first time both the finite DM temperature corrections and the excited states, we obtained an excellent agreement with the observed data (see Figure 2), suggesting that large quantities of baryons are not essential to fit RCs in our model. This precludes the necessity of including large amounts of gas, stars, and feedback processes to flatten the inner regions of RCs. Due to the accurate fits obtained, we expect that adding only the observed amount of baryons will be enough to reach perfect agreement with the RC observations and the observed luminosity. This will be verified in a future work.

Regarding the second problem of fitting the maximum of the RC and the outer regions at the same time, we note from Figure 2 that we no longer have such a problem, in contrast to previous works (Harko 2011; Harko & Madarassy 2011; Robles & Matos 2012). The difference is mainly due to the combination of states in halos. We can estimate a lower bound for j, the minimum excited state necessary to agree with the

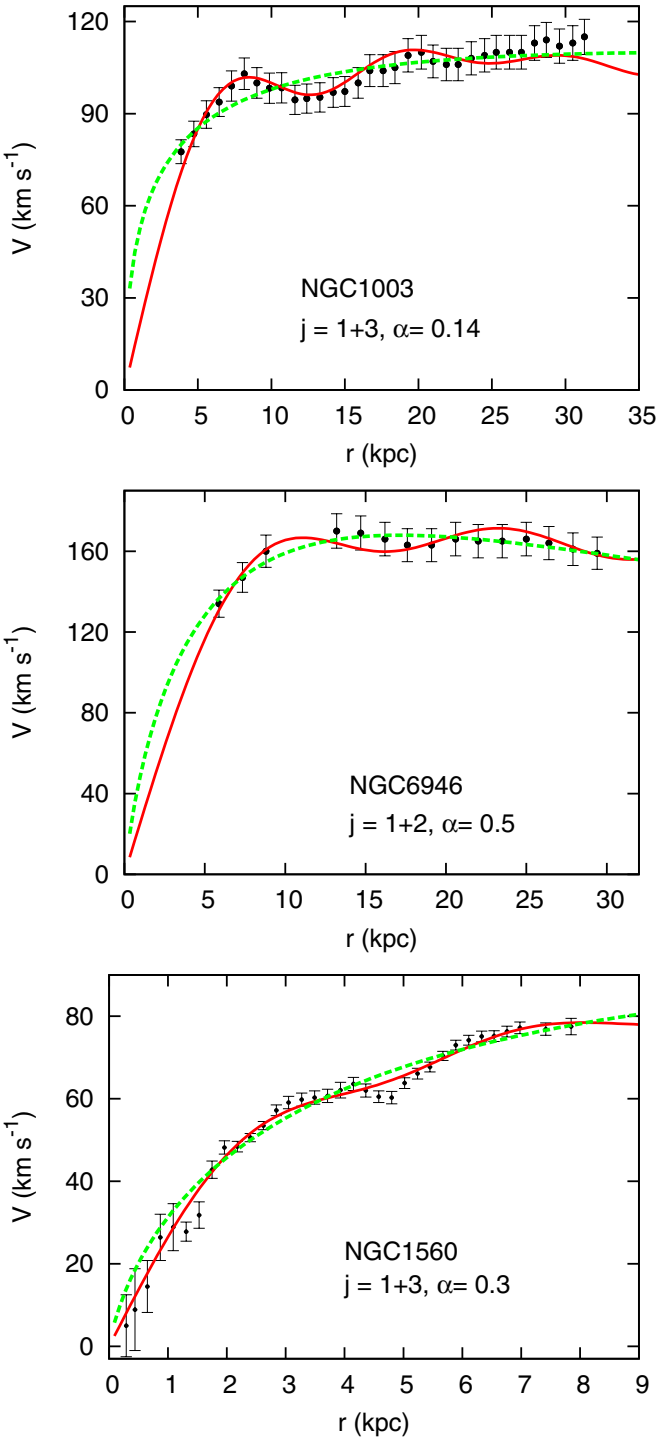

Figure 2. RC fits to three LSB galaxies. Top panel: NGC 1003, middle panel: NGC 6946, and bottom panel: NGC 1560. Solid lines (red in the online version) are the fits using the SFDM model, the dashed line (green in the online version) represents Einasto's fits, and the points are the observational data. In NGC 1560 we see that the dip at $r \approx 5$ kpc is reproduced more accurately in the SFDM profile. The Einasto fits show different values of α in each galaxy, suggesting a non-universality in the DM halos; the same is concluded in the SFDM model.

(A color version of this figure is available in the online journal.)

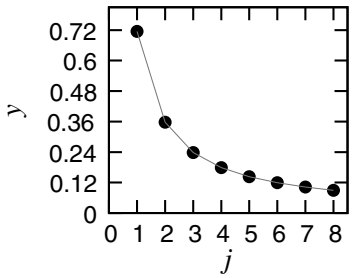

Figure 3. Relation between y and j obtained by solving Equation (23). Note that for halos with large exited states (large j), the first maximum is attained at a smaller y for a fixed radius.

data up to the last measured point, with the following rule of thumb: we find the value of y by identifying from the RC the last measured point as R and the first maximum (first visible peak) as $r^1_{\rm max}$. Then, we look for the closest value of j associated with this y in Figure 3 (the values in Figure 3 are determined by Equation (23)). This provides us with the dominant state in the center of the galaxy, and at the same time, provides us with the minimum state required to fit current observations. It is a lower bound because upcoming observations might go beyond R, and in that case, R will increase and y will decrease, implying larger values of j.

Finally, we see from Figure 2 that the Einasto fits are in general agreement in the outer regions, but that the wiggles cannot be reproduced with DM alone. In fact, if we want to reproduce the oscillations seen in the high-resolution RCs with a non-oscillatory DM profile (NFW, Einasto's, Burkert's, etc.), we must include the gas and star dynamics in the simulations (Famaey & McGaugh 2012). It would be interesting to show the stability of the oscillations after including baryons, as this might be a challenging task in LSB galaxies due to their low-gas surface density.

In addition to the fact that the fits to the observations made with the Einasto profile are good, except for the wiggles and possibly the central region, we note that the parameter α changes for each galaxy. As noted in previous works (Merrit et al. 2006; Navarro et al. 2010; Jin & Suto 2000; Gentile et al. 2007), the change in α implies that halos do not possess a universal profile, i.e., if we take the Einasto profile to be the best representation of the simulated DM halos in a CDM environment, then we should expect to see a non-universality in the halos of galaxies, and this is exactly the same result we have obtained directly from the SFDM model, but without assuming a priori a DM density profile.

4. CONCLUSIONS

In this paper, we obtained a physically motivated extension of the SFDM model that includes DM temperature corrections to the first loop in perturbations. We propose a Z_2 spontaneous symmetry break of a real scalar field to be a new mechanism that forms early DM halos. When the real scalar field rolls down to the minimum of the potential, the perturbations of the field can form and grow. We give an exact analytic solution for a static SF configuration, which in the SFDM model represents a DM halo. This solution naturally presents a flat central density profile, and it can accommodate more than just the ground state, as now the temperature $T \neq 0$. This solves previous discrepancies in rotation curve fits at $T = 0$, for instance, the problem of having a constant halo radius for all galaxies and, in the case of large galaxies, it is not possible to fit at the same time the inner and outermost regions of RCs. Aside from giving a solution to these two disagreements, we mention why it does not seem necessary to include large amounts of feedback to fit and reproduce the inner core and "wiggles" found in high-resolution RCs. Also, the model can be tested with high-redshift observations, as the SF model predicts initial core profiles as opposed to the initially cuspy ones found in CDM simulations, which are expected to flatten due to the redistribution of DM via astrophysical processes. Finally, both the Einasto and SFDM RC fits suggest the non-universality of DM halos, though the latter claim is still not final and further work has to be done in such direction. We strongly believe that further exploration of the SFDM model looks like a promising means to unravel the mystery of DM.

This work was supported in part by DGAPA-UNAM grant IN115311 and by CONACyT Mexico grant 49865-E.

REFERENCES

Avila-Reese, V., Colín, P., Valenzuela, O., D'Onghia, E., & Firmani, C. 2001, ApJ, 559, 516
Balakrishna, J., Seidel, E., & Suen, W. M. 1998, PhRvD, 58, 104004
Bernal, A., Barranco, J., Alic, D., & Palenzuela, C. 2010, in AIP Conf. Proc. 1083, Invisible Universe, ed. J.-M. Alimi & A. Füzfa (Melville, NY: AIP), 20
Böhmer, C. G., & Harko, T. 2007, JCAP, JCAP06(2007)025
Broeils, A. H. 1992, A&A, 256, 19
Brook, C. B., Stinson, G., Gibson, B. K., Wadsley, J., & Quinn, T. 2012, MNRAS, 424, 1275
Burkert, A. 1995, ApJ, 447, L25
Cembranos, J. A. R., Feng, J. L., Rajaraman, A., & Takayama, F. 2005, PhRvL, 95, 181301
Chavanis, P. H. 2011, PhRvD, 84, 043531
Colpi, M., Shapiro, S. L., & Wasserman, I. 1986, PhRvL, 57, 2485
Dalfovo, F., Giorgino, S., Pitaevskii, L. P., & Stringari, S. 1999, RvMP, 71, 463
Davé, R., Spergel, D. N., Steinhardt, P. J., & Wandelt, B. D. 2001, ApJ, 547, 574
de Blok, W. J. G. 2010, AdAst, 2010, 789293
de Blok, W. J. G., McGaugh, S. S., Bosma, A., & Rubin, V. C. 2001, ApJL, 552, 23
De Felice, A., & Tsujikawa, S. 2010, Living Rev. Rel., 13, 3
Famaey, B., & McGaugh, S. S. 2012, LRR, 15, 10
Gentile, G., Baes, M., Famaey, B., & Van Acoleyen, K. 2010, MNRAS, 406, 2493
Gentile, G., Tonini, C., & Salucci, P. 2007, A&A, 467, 925
Gleiser, M. 1988, PhRvD, 38, 2376
Graham, A. W., Merrit, D., Moore, B., Diemand, J., & Terzić, B. 2006, ApJ, 132, 2701
Governato, F., Brook, C., Mayer, L., et al. 2010, Natur, 463, 203
Governato, F., Zolotov, A., Pontzen, A., et al. 2012, MNRAS, 422, 1231
Guo, Q., White, S., Li, C., & Boylan-Kolchin, M. 2010, MNRAS, 404, 1111
Guzmán, F. S., & Matos, T. 2000, CQGra, 17, L9
Harko, T. 2011, MNRAS, 413, 3095
Harko, T., & Madarassy, E. J. M. 2011, JCAP, JCAP01(2011)020
Hu, W., Barkana, R., & Gruzinov, A. 2000, PhRvL, 85, 1158
Jin, Y. P., & Suto, Y. 2000, ApJL, 529, 69
Kain, B., & Ling, H. Y. 2010, PhRvD, 82, 064042
Kuzio de Naray, R., & Kaufmann, T. 2011, MNRAS, 414, 3617
Kuzio de Naray, R., Martinez, G. D., Bullock, J. S., & Kaplinghat, M. 2010, ApJL, 710, 161
Kuzio de Naray, R., & Spekkens, K. 2011, ApJ, 741, L29
Kolb, E., & Turner, M. 1987, The Early Universe (Reading, MA: Addison-Wesley)
Lora, V., Magaña, J., Bernal, A., Sánchez-Salcedo, F. J., & Grebel, E. K. 2012, JCAP, JCAP02(2012)011
Macciò, A. V., Stinson, G., Brook, C. B., et al. 2012, ApJL, 744, 9
Magaña, J., & Matos, T. A. 2012, JPhCS, 378, 012012
Magaña, J., Matos, T., Suárez, A., & Sánchez-Salcedo, F. J. 2012, JCAP, JCAP10(2012)003
Matos, T., & Ureña-López, L. A. 2001, PhRvD, 63, 063506
Matos, T., & Ureña-López, L. A. 2007, GReGr, 39, 1279
Matos, T., Vázquez-González, A., & Magaña, J. 2009, MNRAS, 393, 1359

McGaugh, S. S. 2005, ApJ, 632, 859
McGaugh, S. S., Bothun, G. D., & Schombert, J. M. 1995, AJ, 110, 573
Merrit, D., Graham, A. W., Moore, B., Diemand, J., & Terzić, B. 2006, ApJ, 132, 2685
Milgrom, M. 2010, AIP Conf.Proc. 1241, Invisible Universe, ed. J.-M. Alimi & A. Füzfa (Melville, NY: AIP), 139
More, S., va den Bosch, F. C., Cacciato, M., et al. 2011, MNRAS, 410, 210
Navarro, J. F., Ludlow, A., Springel, V., et al. 2010, MNRAS, 402, 21
Oh, S. H., de Blok, W. J. G., Brinks, E., Walter, F., & Kennicutt, R. C., Jr. 2011, AJ, 141, 193
Rindler-Daller, T., & Shapiro, P. 2012, MNRAS, 422, 135
Robles, V. H., & Matos, T. 2012, MNRAS, 422, 282
Rodríguez-Montoya, I., Magaña, J., Matos, T., & Pérez, L. A. 2010, ApJ, 721, 1509
Romano-Díaz, E., Shlosman, I., Hoffman, Y., et al. 2008, ApJ, 685, L105
Sanders, R. H. 2009, AdAst, 2009, 752439
Sawala, T., Scannapieco, C., & White, S. 2012, MNRAS, 420, 1714
Siddhartha, F. G., & Ureña-López, L. A. 2003, PhRvD, 68, 024023
Sin, S. J. 1994, Phys. Rev. D, 50, 3650
Spergel, D. N., & Steinhardt, P. J. 2000, PhRvL, 84, 3760
Stinson, G. S., Brook, C., Prochaska, J. X., et al. 2012, MNRAS, 425, 1270
Strigari, L. E., Kaplinghat, M., & Bullock, J. S. 2007, PhRvD, 75, 061303
Suárez, A., & Matos, T. 2011, MNRAS, 416, 87
Swaters, R. A., Madore, B. F., & Trewhella, M. 2000, ApJL, 531, 107
Ureña-López, L. A., & Bernal, A. 2010, PhRvD, 82, 123535
Valdez, A. S., Becerril, R., & Ureña-López, L. A. , CQGra, 29, 065021
van Eymeren, J., Trachternach, C., Koribalski, B. S., & Dettmar, R. J. 2009, A&A, 505, 1
Villaescusa-Navarro, F., & Dalal, N. 2011, JCAP, JCAP03(2011)024
Yoshida, N., Springel, V., White, S. D. M., & Tormen, G. 2000, ApJ, 544, L87
Zavala, J., Jing, Y. P., Faltenbacher, A., et al. 2009, ApJ, 700, 1779
Zinner, N. T. 2011, PRI, 2011, 734543